ELECTRONIC SUPPLEMENTARY INFORMATION

Solution synthesis of few-layer WTe_2 and $Mo_xW_{1-x}Te_2$ nanostructures

Yifan Sun[ad], Kazunori Fujisawa[bd], Mauricio Terrones[abcd]*, and Raymond E. Schaak[ad]*

[a] Department of Chemistry and Materials Research Institute, [b] Department of Physics, [c] Department of Materials Science and Engineering, and [d] Center for 2-Dimensional and Layered Materials, The Pennsylvania State University, University Park, PA 16802

E-mail: res20@psu.edu, mut11@psu.edu

Supplementary Tables

Table S1. Experimental parameters for the synthesis of $Mo_xW_{1-x}Te_2$ nanostructures.

$Mo_xW_{1-x}Te_2$	WCl_6 / mmol	$MoCl_6$ / mmol	Te / mmol
T_d-WTe_2	0.15	0	1.2
x = 0.19	0.8×0.15	0.2×0.15	1.2
x = 0.39	0.6×0.15	0.4×0.15	1.2
x = 0.52	0.4×0.15	0.6×0.15	1.2
x = 0.80	0.2×0.15	0.8×0.15	1.2
1T′-$MoTe_2$	0	0.15	1.2

Supplementary Figures

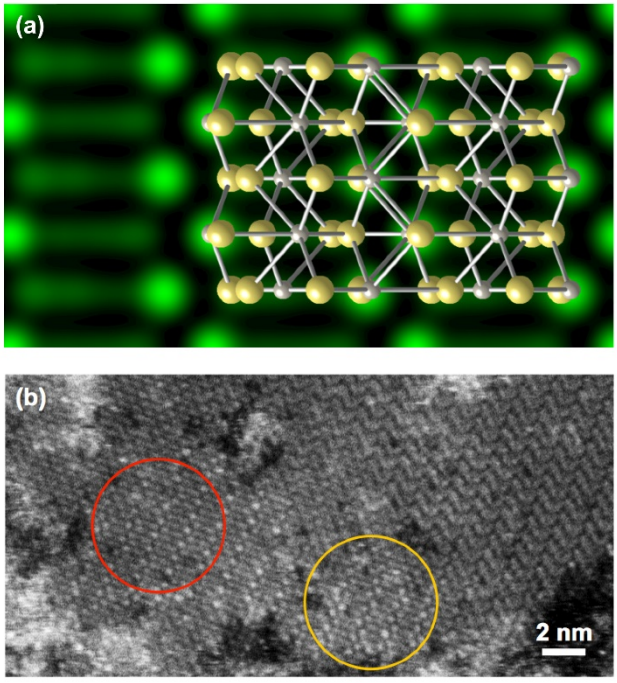

Fig. S1 (a) Simulated ADF images of bilayer WTe_2 with T_d stacking. (b) 2H- and 2H′-analogous stacking of WTe_2 layers, highlighted by red and yellow circles, respectively.

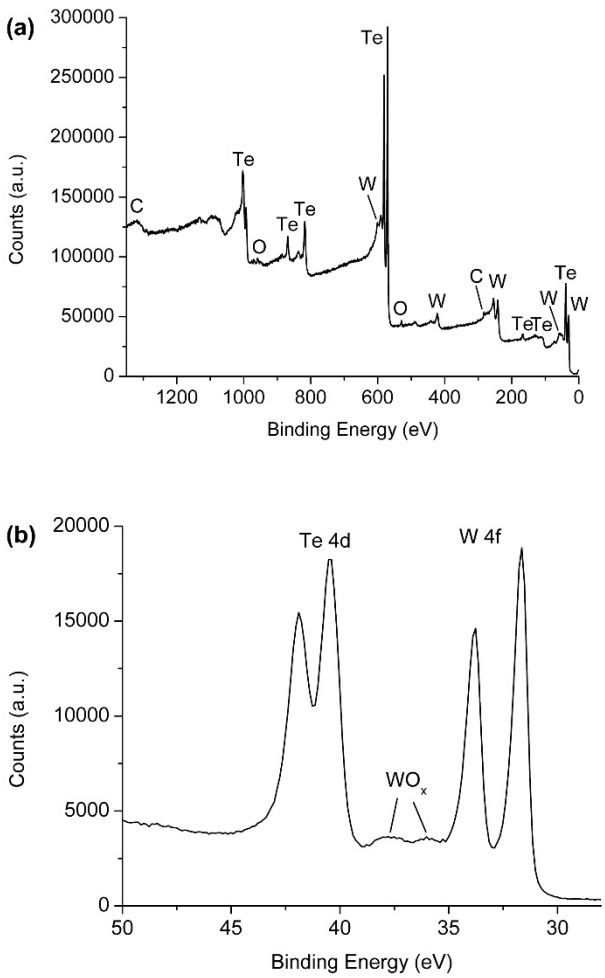

Fig. S2 (a) XPS survey scan for the as-prepared WTe_2 nanostructures, showing the presence of W, Te, C, and O. (b) XPS spectra for the WTe_2 nanostructures with (b) Te 4*d* and (c) W 4*f* regions. The minor shoulder peaks at higher binding energy could be due to potential oxidation introduced during the washing process.

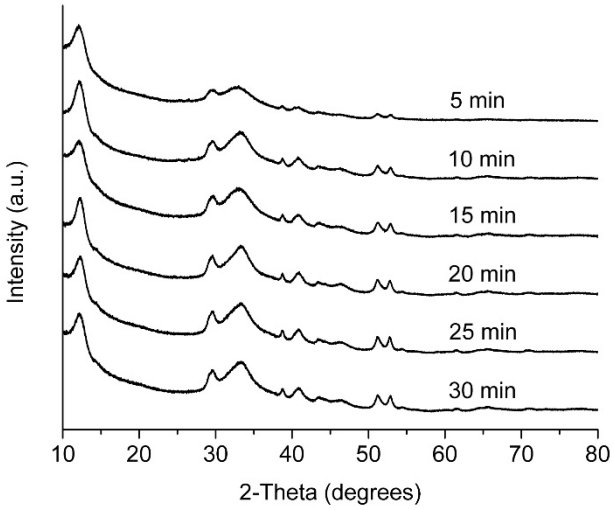

Fig. S3 Powder XRD patterns of the WTe_2 nanostructures obtained after (a) 5 min, (b) 10 min, (c) 15 min, (d) 20 min, (e) 25 min, and (f) 30 min.

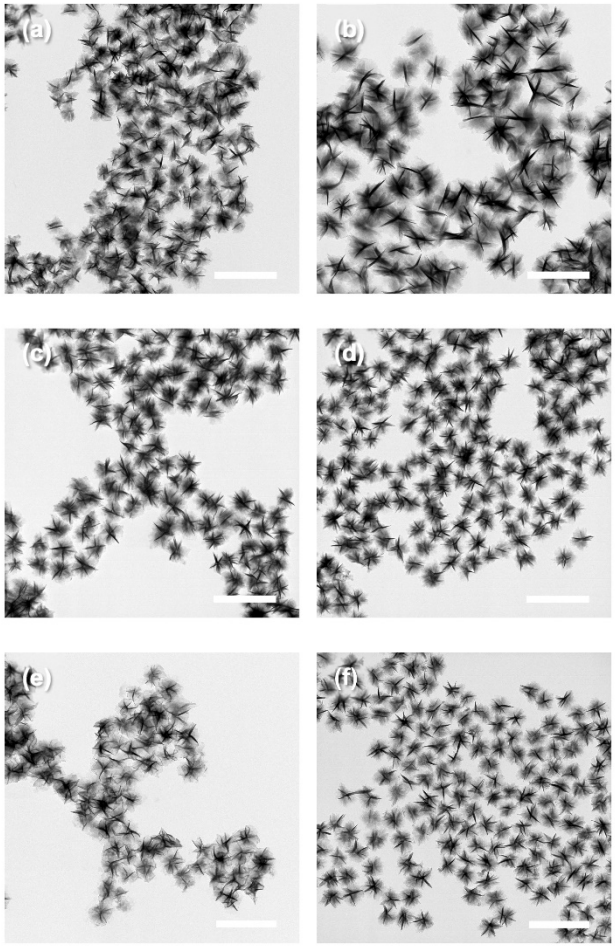

Fig. S4 TEM images (500 nm scale bars) for $Mo_xW_{1-x}Te_2$ with x = (a) 0, (b) 0.19, (c) 0.39, (d) 0.52, (e) 0.80 and (f) 1.

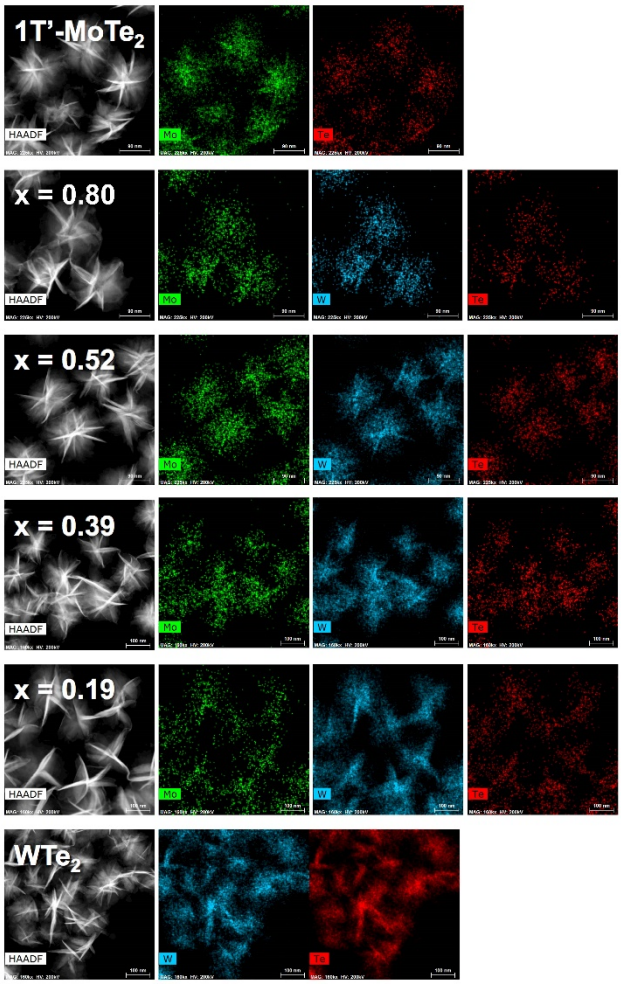

Fig. S5 HAADF-STEM images and corresponding STEM-EDS element maps for the $Mo_xW_{1-x}Te_2$ nanostructures, indicating a uniform distribution of Mo, W, and Te.

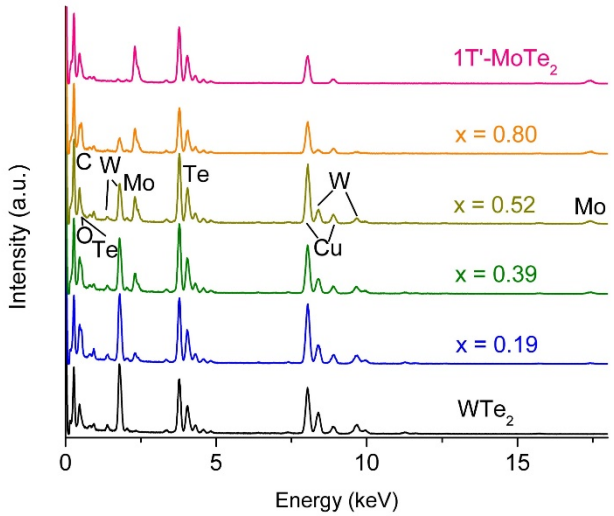

Fig. S6 EDS spectra for the $Mo_xW_{1-x}Te_2$ nanostructures. The Cu signal comes from the Cu TEM grids.